# Looking at Light

James Amarel and Ben Miller

March 17, 2017

## 1 Goal

We investigate an Ocean Optics spectrometer and its automated ability to determine the properties of electromagnetic radiation. We will first calibrate the spectrometer by observing the Helium spectrum. Then we use our accurate calibration to explore the spectra of Hydrogen and Mercury. Lastly, we observe the black body radiation of a heated tungsten filament and use the Planck distribution to predict the filament temperature.

## 2 Introduction/Background

The characteristic electromagnetic radiation from a substance can be used to understand a great variety of physical phenomena. For example, we can infer a molecular/atomic structure, or use statistical mechanics to predict the substance temperature, and in some cases determine the relative velocity of an object. Modern technology no longer requires the labor intensive process of manual data retrieval and processing when doing spectral analysis. In principle, spectrometers rely on a dispersive medium to exploit a wavelength dependent refractive index [1]. Instead of visually recording the angle of refraction, the process is automated by monitoring the entire spectrum with a CCD array. The camera array corresponds to discrete pixel numbers that correspond to a measured wavelength and can report an intensity value.

# 3 Calibration

## 3.1 Description

Our spectrometer came equipped with a factory default calibration that is linked with computer based spectra analysis software. A built-in factory calibration relates each pixel value to a corresponding wavelength, but the accuracy of this calibration deteriorates with time. So instead, we will observe the band spectra of Helium with the spectrometer and use the accepted wavelength values to build a more accurate calibration relation. We use the first nine known wavelengths of the Balmer series to obtain a second order polynomial fit for the wavelength as a function of the pixel value,

$$\lambda = a + bp + cp^2 \tag{1}$$

where $\lambda$ is the wavelength, $p$ is the pixel number, and $a, b, c$ are fit parameters. Once each free parameter is determined, we can use our calibration tool to compute the wavelength corresponding to each pixel value for any radiation source.

## 3.2 Procedure and Data

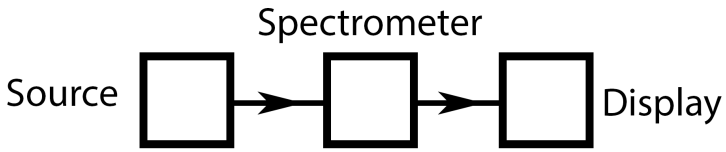


Figure 1: Block diagram of the experimental process. A source emits electromagnetic radiation that is collected by the spectrometer and displayed via computer software.

To obtain the calibration data, we placed the spectrometer's optical input fiber adjacent to a Helium discharge tube. Then, as seen in 3.2, the spectral analysis software displays the pixel intensity vs pixel number. This plot reveals low intensity values across all pixels, except those localized near pixels that are apart of the Helium spectrum. Spectral lines produce sharp peaks that are vastly greater in intensity than the low noise level, making them easily distinguishable. We recorded the pixel number for the nine largest peaks of our observed Helium spectrum, which can be seen in the Table 1.

Table 1: Recorded pixel numbers for the Helium spectrum.

| Pixel Value | 1865 | 1753 | 1554 | 1152 | 733 | 688 | 588 | 474 | 200 |
|---|---|---|---|---|---|---|---|---|---|

The peaks seen on screen usually had a width of a few pixels and fluctuated with time. To account for this we froze the spectrometer display and took measurements of the central pixel number. We expect these measurements to be accurate within $\pm 0.5$ pixel.

## 3.3 Analysis and Discussion

When recording the peak pixels numbers, we used the computer reported wavelength value to ensure we were observing the known Helium spectrum. But the computer reported wavelengths are only approximate, so a Matlab fitting algorithm is supplied the data from Table 1 and the wavelength relation of Equation 1, which results in the fit seen in Figure 3.3.

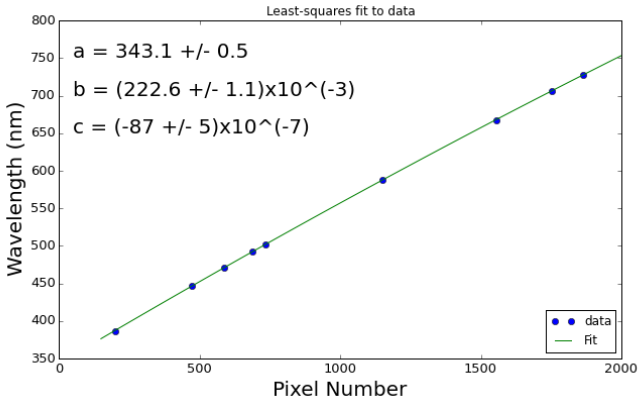


Figure 2: Fitting results after calibrating with Equation 1 with the known Helium spectrum and the data in Table 1

Where a,b,c are the fitting parameters from Equation 1. Then we use the calibrated parameters to determine the true measured wavelengths, as seen in Table 2.

To determine the accuracy of the calibration, we compute the root mean square deviation of the measured wavelengths from the accepted values. Then, the best estimate of uncertainty in $\lambda$ is found from the square root of

Table 2: Comparison of our measured wavelengths of the Helium spectrum with the accepted wavelengths.

| $\lambda$ Measured (nm) | $\lambda$ Accepted (nm) | $\lambda$ Measured (nm) | $\lambda$ Accepted (nm) |
|---|---|---|---|
| 727.9 | 728.13 | 492.1 | 492.19 |
| 706.5 | 706.52 | 471.0 | 471.31 |
| 668.0 | 667.81 | 446.7 | 447.14 |
| 588.0 | 587.57 | 387.3 | 386.86 |
| 501.6 | 501.57 | | |

the average of all squared deviations. This results in $\delta\lambda = 0.3$ nm. which agrees with the fact that all measured wavelengths lie within 0.6 nm of the corresponding accepted value.

# 4 Resolution

## 4.1 Description

Next, we investigate the resolution of our spectrometer by determining the instrumental line-width through observation of a mono-energetic laser. The spectral analysis program displays intensity vs pixel value, but many peaks have a thickness of a few pixels. Therefore, two spectra lines can only be resolved if the distance between their centers is greater than the full width half mass of each peak.

## 4.2 Procedure and Data

To determine the instrumental line-width, we use an HeNe laser of known wavelength $\lambda = 632.82$ nm and observe the laser in reflection to avoid damaging the spectrometer. The laser has a single peak centered about pixel #1378, which corresponds to a measured wavelength of 632.81 nm. This result is in great agreement with the laser specifications. We found the FWHM by visually identifying the pixel number for the half mass point on each side of the central peak. We found the full width at half mass to be 7 pixels, from pixel #1375 to pixel #1382. And again we estimate that these pixels values are correct within a half pixel.

Next, we observed the spectra for three hand held LED's of different color.

For each laser we recorded the peak pixel value and FWHM of the spectra, which are seen in Table 3. As expected, the LED's produce a much broader spectrum than the HeNe laser, the FWHM for LED's is around 60 pixels, which is much larger than found for the laser.

Table 3: Peak pixel value and FWHM values for three hand held LED's.

| LED Color | Peak Pixel | Left FWHM Pixel | Right FWHM Pixel |
|---|---|---|---|
| Red | 1386 | 1340 | 1418 |
| Green | 814 | 755 | 896 |
| Blue | 540 | 490 | 625 |

## 4.3 Analysis and Discussion

The instrumental line width of our spectrometer is calculated from the calibration equation and the full width half mass points of the HeNe laser. We find the FWHM is 1.4 nm, which is about five times greater than the experimental uncertainty. It is important not to confuse the experimental uncertainty with the spectrometer resolution or instrumental line width. The instrumental line width is effectively the smallest division increment that the instrument can display (precision), but our uncertainty contains information about the accuracy as well, and the uncertainty doesn't determine our ability to resolve separate peaks.

The peak pixel value for each LED corresponds to the approximate known values for red, green, and blue light. From Table 3, we calculated a blue wavelength of 460 nm, a green wavelength of 520 nm, and a red wavelength of 634 nm, although these can only be considered the approximate central wavelength. From the FWHM data we see that the LED's have a fairly large spread of about 30 nm, which is quite a difference from the HeNe laser. The LED spectrum also weren't very Gaussian in nature, often the distribution heavily favored one side of the peak.

# 5 Hydrogen

## 5.1 Description

An automated spectrometer can be quickly and easily used to determine the spectral lines of an atom or molecule. As we saw in the Atomic Spectra lab, the emitted wavelength of photons from Hydrogen go as

$$\frac{1}{\lambda} = C(1/m^2 - 1/n^2) \tag{2}$$

where C is a constant related to the Rydberg energy, n is the principle quantum number of the initial state, and m is the final state.

## 5.2 Procedure and Data

To measure the spectral lines of Hydrogen, we used a Hydrogen discharge tube and placed the spectrometer input near enough to gather a spectrum that was not saturated, but also allowed us to distinguish all the peaks. Then we measured the peak pixel value of each spike corresponding to a transition of the Balmer series, which can be found in Table 4.

Table 4: Recorded pixel values for the Hydrogen spectrum and their corresponding wavelength.

| Peak Pixel | $\lambda_{meas}$ |
|---|---|
| 1495.5 | 651.1 |
| 659 | 486.1 |
| 412 | 434.1 |
| 300 | 410.2 |
| 238 | 396.9 |

## 5.3 Analysis and Discussion

First, we calculated the measured wavelengths from our peak pixel values and the calibration relation. This results in the measured wavelengths as seen in Table 4. From the measured wavelengths we used an optimization routine to estimate the values of the $C$ and $m$ parameters as seen in Equation 2.

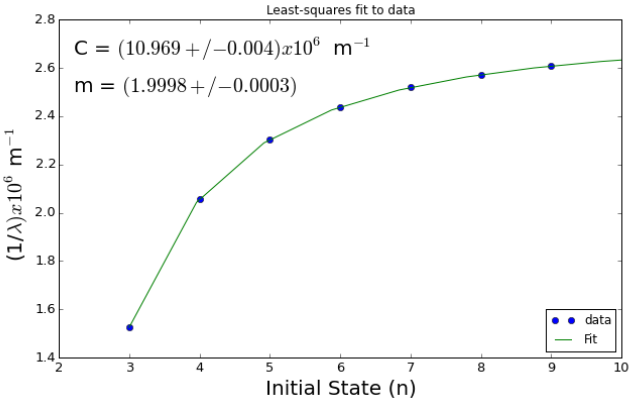


Figure 3: The optimization results of fitting Equation 2 with our measured Hydrogen spectrum in the Balmer series.

The fitting results, as seen in Figure 5.3 gives a great result for the final principle quantum number, $m$, which is restricted to whole numbers and is equal to 2 in Balmer lines. Additionally the fitting routine provides a value for $C$, which is equivalent to $E_r/hc$, where $E_r$ is the Rydberg energy, $h$ is Planck's constant, and $c$ is the speed of light. Then the accepted value of $C$ is $10.9737x10^6$ $m^{-1}$, which agrees with our measured value of $(10.969 \pm 0.004)x10^6$ $m^{-1}$.

# 6 Mercury

## 6.1 Description

The Mercury spectrum is more complex than the Hydrogen spectrum, but can be measured in the same manner. A manual spectrometer can make it difficult to distinguish between spectral lines that are very near in wavelength, but our spectrometer should have no issues distinguishing any of the predicted Mercury lines. We can investigate the precision of the spectrometer by focusing on the wavelengths corresponding to the yellow doublet of Mercury's emission spectrum.

## 6.2 Procedure and Data

We used the same procedure as in the Hydrogen spectrum to observe the spectra of a Mercury discharge tube. The data and corresponding measured wavelengths for our Mercury observations are seen in Table 5. Even though the two doublet lines are quite similar in wavelength, the peak to peak separation is about seven times the instrumental uncertainty and so there is no difficulty in resolving them.

Table 5: Measured pixel numbers for the peaks of Mercury's yellow doublet and the measured corresponding wavelengths.

| Peak Pixel | $\lambda_{meas}$ |
|---|---|
| 1101 | 577.1 |
| 1111 | 579.2 |

## 6.3 Analysis and Discussion

The peak to peak separation of the yellow doublet lines was observed to be 2.1 nm, which is larger than the spectrometer resolution and incredibly simple to obtain. These values are considerably different than the values of 571.9 nm and 570.2 nm that we recording when measuring a similar Mercury source with a manual spectrometer. It is reasonable to expect that the automated spectrometer eliminated a large source of systematic error and thus can give a more reliable data point.

# 7 White Light

## 7.1 Description

All of the previously observed spectra contain white noise from the lab environment, which makes relative intensity measurements between wavelengths meaningless. To fix this issue, we will use a continuous source of well known radiation and perform another spectrometer calibration. A black body radiation source emits a spectrum that can be predicted by the Planck distribution. With a special irradiance mode that is built into the software we can filter out the background noise and observe only the black body spectrum if

we know the temperature of the radiating object. The Planck black body curve represents the energy density (of radiation) per unit photon energy. Then, the peak of the spectrum corresponds to the photon wavelength of greatest relative intensity [2]. For short wavelengths the Planck curve can be approximated by

$$I_\lambda = C\lambda^{-5} e^{\frac{-hc}{\lambda k T}} \tag{3}$$

where $I_\lambda$ is the intensity at $\lambda$, $c$ is the speed of light, $T$ is the temperature, and $C$ is a constant whose value is unnecessary for our investigation.

## 7.2 Procedure and Data

We used a light bulb made from a glowing tungsten filament as an approximate reference black body. In order to calibrate the spectrometer to our bulb source, we used an optical pyrometer to determine the temperature of the bulb when it is being supplied full power. We found the temperature of the filament to be 2350 celsius. Then we entered the color temperature into the spectral analysis software and used the program to monitor radiation when the bulb was on and off. Once these steps are completed, irradiance mode allows one to view solely the radiation emitted by the bulb.

When the bulb was supplied full power, the program displayed a spectrum that closely resembled a black body curve in the region with wavelengths on the order of microns. We were unable to see the peak of the curve because the spectrometer was saturated in that region. Instead of focusing on the peak, we measured the pixel intensity at $\lambda = 800$ nm and $\lambda = 600$ nm. The spectra analysis software reports an arbitrary pixel intensity value of 10.1 for $\lambda = 600$ nm and intensity 26.3 for $\lambda = 800$ nm, we will later take the ratio of these values to avoid the issue of unknown units.

Next, we use a variable power source to supply the light bulb with half power and measure the pixel intensity values at the same wavelengths. We recorded an intensity of 0.78 for $\lambda = 600$ nm and 3.1 $\lambda = 800$ nm. Finally, we used an optical pyrometer to determine the bulb temperature as 1880 Celsius when it is being supplied half power. We can see that dropping the initial temperature of 2623K to nearly 80% of its value produces about a 10-fold reduction in radiation intensity.

### 7.3 Analysis and Discussion

The predicted intensity ratio as predicted by Equation 3 is $I_{800nm}/I_{600nm} = 2.33$, which is in decent agreement with our value $I_{800nm}/I_{600nm} = 26.3/10.1 = 2.6$. We expect that this 10% discrepancy is sufficient enough to produce accurate results. When the bulb power was lowered to 50%, our measured intensity ratio went to $I_{800nm}/I_{600nm} = 3.1/.78 = 3.97$. Then we invert Equation 3 to solve for the temperature necessary to produce the ratio $I_{800nm}/I_{600nm}3.97$ and find $T = 1856$ Celsius. Therefore we measured the temperature of our bulb at half power with two different methods, the optical pyrometer gave $T = 1880$, which agrees with our black body spectrum measurement of $T = 1856$.

## 8 Conclusion

Our modern spectrometer allowed us to measure many quantities at a quicker rate and with higher precision and accuracy than manual devices. We recorded the Helium spectrum with an estimated uncertainty of 0.3 nm, where all of our data lay within one standard deviation of the accepted value. The Helium observations allowed us to build a calibration relation and then we were able to further investigate the limitations of the instrumental resolution. By measuring the full width at half mass of a monochromatic laser source, we determined the instrumental line width to be 1.4 nm. Then we observed the discharge tube spectrum of Hydrogen and Mercury. Additionally we used our measured wavelengths for Hydrogen to determine the Rydberg constant $(10.969 \pm 0.004)x10^6$ m$^{-1}$, which is very accurate according to the accepted value. Our final measurement was of the temperature of a glowing tungsten light bulb. By taking reference data, we were able to subtract out the background noise and view only the filaments nearly black body spectrum. Clearly a modern spectrometer is a versatile measuring device that can be used to investigate many quantities more precisely than was possible in the past, and spectral analysis programs can be adapted to monitor samples in ways that were not previously possible.

# References

[1] Adrian C. Melissinos. *Experiments in Modern Physics*. Academic Press, 2003.

[2] Daniel V. Schroeder. An Introduction to Thermal Physics, 1999. ISSN 00029505.